

Safety Guarantees for Neural Network Dynamic Systems via Stochastic Barrier Functions

Rayan Mazouz^{1*}, Karan Muvvala^{1*}, Akash Ratheesh¹, Luca Laurenti², Morteza Lahijanian¹

¹ Department of Aerospace Engineering Sciences, University of Colorado Boulder, USA

² Delft Center for Systems and Control, Delft University of Technology, The Netherlands

{rayan.mazouz, karan.muvvala, akash.ratheesh, morteza.lahijanian}@colorado.edu
{l.laurenti}@tudelft.nl

* Equal Contribution

Abstract

Neural Networks (NNs) have been successfully employed to represent the state evolution of complex dynamical systems. Such models, referred to as NN dynamic models (NNDMs), use iterative noisy predictions of NN to estimate a distribution of system trajectories over time. Despite their accuracy, safety analysis of NNDMs is known to be a challenging problem and remains largely unexplored. To address this issue, in this paper, we introduce a method of providing safety guarantees for NNDMs. Our approach is based on stochastic barrier functions, whose relation with safety are analogous to that of Lyapunov functions with stability. We first show a method of synthesizing stochastic barrier functions for NNDMs via a convex optimization problem, which in turn provides a lower bound on the system's safety probability. A key step in our method is the employment of the recent convex approximation results for NNs to find piece-wise linear bounds, which allow the formulation of the barrier function synthesis problem as a sum-of-squares optimization program. If the obtained safety probability is above the desired threshold, the system is certified. Otherwise, we introduce a method of generating controls for the system that robustly maximizes the safety probability in a minimally-invasive manner. We exploit the convexity property of the barrier function to formulate the optimal control synthesis problem as a linear program. Experimental results illustrate the efficacy of the method. Namely, they show that the method can scale to multi-dimensional NNDMs with multiple layers and hundreds of neurons per layer, and that the controller can significantly improve the safety probability.

1 Introduction

Safety is a major concern for autonomous dynamical systems, especially in *safety-critical* applications. Examples include UAVs, autonomous cars, and surgical robots. To this end, various methods are developed to provide safety guarantees for such systems [1–3]. Most of these methods, however, assume (simple) analytical models, which are often unavailable or too expensive to obtain due to complexity (nonlinearities) in real-world systems [4]. This has given rise to recent efforts to harvest the representational power of *neural networks* (NNs) to predict how the state of a system evolves over time, referred to as *NN dynamic models* (NNDMs) [5, 6]. Despite their efficient and accurate representation of realistic dynamics, it has been difficult to make formal claims about the behavior of NNDMs over time. This poses a major challenge in safety-critical domains: *how to provide safety guarantees for NNDMs?*

In this paper, we propose a framework to provide safety certificates for NNDMs. The approach is based on stochastic barrier functions [7, 8], whose role for safety is analogous to that of Lyapunov functions for stability, and which can guarantee forward invariance of a safe set. Specifically, we

show a method of synthesizing barrier functions for NNDMs via an efficient convex optimization method, which in turn provides a lower bound on the safety probability of the system trajectories. The benefit of our approach is that it does not require unfolding of the NNDM to compute this probability; instead, we base our reasoning on non-negative super-martingale inequalities to bound the probability of leaving the safe set. The key to this is to utilize the recent convex approximation results for NNs to obtain piece-wise linear bounds, and a formulation of the optimization problem that enables the use of efficient solvers. If the obtained safety probability is above a desired threshold, the system can be certified. For the cases that such safety certificates cannot be provided, we introduce a method of generating controls for the system, which robustly maximizes the safety probability in a minimally-invasive manner. We exploit the convexity property of the barrier function to formulate the control synthesis problem as a linear program. Experimental results on various NNDMs trained using state-of-the-art RL techniques [9–11] illustrate the efficacy of the method. Namely, they show that the method can scale to multi-dimensional models with various layers and hundreds of neurons per layer, and that the controller can significantly improve the safety probability.

In summary, this paper makes the following main contributions: (i) a method of computing a lower bound for the safety probability of NNDMs via stochastic barrier functions and efficient nonlinear optimization, thereby providing safety guarantees, (ii) a correct-by-construction control synthesis framework for NNDMs to ensure safety while being *minimally-invasive*, i.e., intervening only when needed, (iii) demonstration of the efficacy and scalability of the framework in benchmarks on various NNDMs with multiple architectures, i.e., multiple hidden layers and hundreds of neurons per layer.

Related Work In recent years, NNs have been successfully employed to model complex dynamical systems [5, 6]. Such models use iterative noisy predictions of an NN to estimate the distribution of the system over time. They provide means of predicting state evolution of the systems that have no analytical form, e.g., soft robotics [12]. In addition, because of their ability to quickly unfold trajectories, NNDMs have been used to enhance controller training in Reinforcement Learning (RL) frameworks [9, 11]. In these works, specifically, a NNDM of the system is trained in closed-loop with an NN controller, which can be concatenated in a single NN representing the dynamics of the closed-loop system. Despite their popularity and increased usage, little work has gone to safety analysis of NNDMs. This paper aims to fill this gap.

Barrier functions provide a formal methodology to prove safety of dynamical systems [13, 14]. The state-of-the-art to find stochastic barrier functions is arguably to rely on Sum-of-Squares (SOS) optimization [8]. Barrier certificates obtained via SOS optimization have been studied for deterministic, uncontrolled nonlinear systems [15], and control-affine stochastic systems [16, 8], as well as for hybrid models [13, 14]. In addition, the control synthesis formulation in this paper relaxes the limitations of the existing SOS methods, which generally leads to a non-convex optimization problem [8], by reducing it to a simple linear program.

Many recent studies have focused on the verification of NNs. However, most of them only aim to provide certification guarantees against adversarial examples [17], with approaches ranging from SMT [18], and convex relaxations [19] to linear programming [20]. Such methods, because of their local nature, cannot be directly employed to perform safety analysis on the entire state space and over the trajectories as required for NNDMs. Another line of work focuses on infinite time horizon safety of Bayesian neural networks [21], or the verification of neural ODEs with stochastic guarantees [22]. They consider neural network controllers with known dynamics [23]. Other methods have been employed for trajectory-level properties of NNs based on solution of the Bellman equations [24], formal (finite) abstractions [25], and mixed integer programming [26], which do not support noisy dynamics. In contrast, our approach supports additive noise and only requires to check static properties on the NN by showing that there exists a function whose composition with the NN forms a stochastic barrier function.

2 Problem Formulation

In this work, we are interested in providing safety guarantees for dynamical systems that are described by NNs. Specifically, we consider the following discrete-time stochastic process whose time evolution is given by iterative predictions of an NN

$$\mathbf{x}_{k+1} = f^w(\mathbf{x}_k) + \mathbf{v}_k, \quad k \in \mathbb{N}, \quad \mathbf{x}_k, \mathbf{v}_k \in \mathbb{R}^n, \quad (1)$$

where f^w is a trained, fully-connected, feed-forward NN with general continuous activation functions, and w represents the maximum likelihood weights. Term \mathbf{v}_k is a random variable modelling an additive noise of stationary Gaussian distribution with zero mean and covariance matrix $R \in \mathbb{R}^{n \times n}$, i.e., the probability density function of \mathbf{v}_k is $\mathcal{N}(\bar{x} \mid 0, R)$.

Remark 1. System (1) can be viewed as a closed-loop system, where f^w is the composition of a NNDM (that represents the open-loop system) with an NN controller. NNDMs such as the one in System (1) are increasingly employed in robotics for both model representation and NN controller training. These models are often obtained by state-of-the-art model-based RL techniques (e.g., [9–11]) or perturbations (step response) of the actual system (e.g., [12]).

The evolution of System (1) can be characterized by the predictive posterior distribution $p_{\mathbf{x}}(\bar{x} \mid x)$, which describes the probability density of \mathbf{x}_{k+1} when $\mathbf{x}_k = x \in \mathbb{R}^n$. This distribution is induced by noise \mathbf{v}_k and hence is Gaussian with mean $f^w(x)$ and covariance R , i.e., $p_{\mathbf{x}}(\bar{x} \mid x) = \mathcal{N}(\bar{x} \mid f^w(x), R)$. For a subset of states $X \subseteq \mathbb{R}^n$ and (initial) state $x \in \mathbb{R}^n$, we call $T(X \mid x) = \int_X p_{\mathbf{x}}(\bar{x} \mid x) d\bar{x}$ the *stochastic kernel* of System (1). From the definition of T it follows that, for a given initial condition $\mathbf{x}_0 = x_0 \in \mathbb{R}^n$, \mathbf{x}_k is a Markov process with a well-defined probability measure \Pr uniquely generated by the stochastic kernel T [27, Proposition 7.45]. For $X_0, X_k \subseteq \mathbb{R}^n$, this probability measure is inductively defined as

$$\Pr[\mathbf{x}_0 \in X_0] = \mathbf{1}_{X_0}(x_0), \quad \Pr[\mathbf{x}_k \in X_k \mid \mathbf{x}_{k-1} = x] = T(X_k \mid x),$$

where indicator function $\mathbf{1}_{X_0}(x_0) = 1$ if $x_0 \in X_0$, otherwise 0. The definition of \Pr allows one to make probabilistic statements over the trajectories of System (1). In this work, we are particularly interested in two main problems: safety certification and safe controller synthesis for System (1).

Problem 1 (Safety Certificate). *Let $X_s \subset \mathbb{R}^n$ and $X_0 \subseteq X_s$ be basic closed semi-algebraic sets representing respectively the safe set and the set of initial states. Denote the probability that the system initialized in X_0 remains in the safe set in the next $N \in \mathbb{N}_{\geq 0}$ steps by*

$$P_s(X_s, X_0, N) = \Pr[\forall x_0 \in X_0, \forall k \leq N, \mathbf{x}_k \in X_s]. \quad (2)$$

Then, given threshold $\delta_s \in [0, 1]$, provide a safety certificate for System (1) by proving that $P_s(X_s, X_0, N) \geq \delta_s$.

Problem 1 seeks to compute the probability that \mathbf{x}_k remains within a safe set, e.g., it avoids obstacles or any undesirable states. Computation of this probability is particularly challenging because System (1) is stochastic and NN (f^w) is generally a non-convex function. The assumption that X_s and X_0 are basic closed semi-algebraic sets is not limiting, as these sets are defined as an intersection of a finite number of polynomial inequalities and, for instance, include convex polytopes and spectrahedra [28].

In the case that a safety certificate cannot be generated, we are interested in synthesizing a controller that *by-design* guarantees safety. To this end, we extend System (1) with an affine input

$$\mathbf{x}_{k+1} = f^w(\mathbf{x}_k) + g\mathbf{u}_k + \mathbf{v}_k, \quad (3)$$

where $g : \mathbb{R}^c \rightarrow \mathbb{R}^n$ is given, $\mathbf{u}_k \in U \subset \mathbb{R}^c$ is a control action, and U is bounded. Our goal is to synthesize a feedback controller $\pi : \mathbb{R}^n \rightarrow U$ such that $\mathbf{u}_k = \pi(\mathbf{x}_k)$ guarantees safety of System (3).

Problem 2 (Safe Control Synthesis). *Let $X_s \subset \mathbb{R}^n$ and $X_0 \subseteq X_s$ be basic closed semi-algebraic sets representing respectively the safe set and the set of initial states, and $N \in \mathbb{N}_{\geq 0}$ a time horizon. Then, given threshold δ_s , synthesize a feedback controller π such that $P_s(X_s, X_0, N, \pi) \geq \delta_s$, where $P_s(X_s, X_0, N, \pi)$ is the safety probability obtained for control-affine System (3).*

Remark 2. *There may exist many possible controllers that are solutions to Problem 2. Since System (1) represents a closed-loop system with a given controller, one may want to specifically synthesize a safety controller that is “minimally-invasive,” i.e., it minimally intervenes to guarantee safety. In Section 5, we elaborate on this notion and introduce methods of generating such controllers.*

Overall Approach Our approaches to Problems 1 and 2 are based on (stochastic) barrier functions. Specifically, we aim to synthesize barrier functions that can serve as a safety certificate by providing a lower bound for P_s . To achieve this, we rely on recent results for local convex relaxation of an NN to find piece-wise linear over- and under-approximations of f^w . This allows us to formulate the problem of finding a stochastic barrier function for System (1) as an SOS optimization problem.

Our (minimally-invasive) control synthesis method (Problem 2) focuses on injecting controls to System (3) only in the regions of the state space that potentially contribute to unsafety of the system. To this end, we exploit two main properties of the barrier function: the required (super-) martingale property and the convexity property of SOS polynomials. The former allows us to design a method of identifying the “unsafe” regions, and the latter enables us to formulate a Linear Programming (LP) optimization problem to find controllers that robustly minimize the probability of unsafety.

Remark 3. For ease of presentation, g in (3) is taken to be a constant, however, we note that the proposed approach can also handle g being a continuous function of x , or even a NN. For the latter, we introduce an interval bound propagation approach in Section 4.1 that allows the computation of upper and lower bounds on $g(x)$, which in turn can be incorporated in the LP optimization formulation in Section 5 for control synthesis (Problem 2) in a straightforward manner.

3 Preliminaries

In this section, we provide a brief background on stochastic barrier functions and non-negative polynomials, which are central components of our framework.

3.1 Stochastic Barrier Functions

Consider stochastic process $\mathbf{x}_{k+1} = F(\mathbf{x}_k, \mathbf{v}_k)$, where $\mathbf{x}_k \in X \subseteq \mathbb{R}^n$, $\mathbf{v}_k \in V \subseteq \mathbb{R}^m$ is a well-defined stochastic process, and $F : X \times V \rightarrow X$ is a locally Lipschitz continuous function. Then, given initial set $X_0 \subset X$, safe set $X_s \subseteq X$, and unsafe set $X_u \subset X$, a twice differentiable function $B : X \rightarrow \mathbb{R}$ is called a *stochastic barrier function* or simply barrier function if the following conditions hold for $\alpha \geq 1$ and $\beta, \eta \in [0, 1]$:

$$B(x) \geq 0 \quad \forall x \in X \quad (4a)$$

$$B(x) \leq \eta \quad \forall x \in X_0 \quad (4b)$$

$$B(x) \geq 1 \quad \forall x \in X_u \quad (4c)$$

$$E[B(F(x, v)) \mid x] \leq B(x)/\alpha + \beta \quad \forall x \in X_s \quad (4d)$$

If such a B exists, then for any $N \in \mathbb{N}_{\geq 0}$, it follows, assuming $\alpha = 1$ without loss of generality, that

$$\Pr[\forall k \leq N, \mathbf{x}_k \in X_s \mid \mathbf{x}_0 \in X_0] \geq 1 - (\eta + \beta N). \quad (5)$$

Intuitively, Conditions (4a)-(4d) allow one to use non-negative super-martingale inequalities to bound the probability that the system reaches the unsafe region. This results in the probability bound in (5) (see [29, Chapter 3, Theorem 3]). A major benefit of using barrier functions for safety analysis is that while Conditions (4b)-(4d) are static properties, they allow one to make probabilistic statements on the time evolution of the system without the need to evolve the system over time.

3.2 Non-negative Polynomials

Synthesis of barrier functions can be formulated as a nonlinear optimization problem. To solve it efficiently via convex programming, we formulate the problem using SOS polynomials, which is a sufficient condition for polynomial non-negativity [30]. This formulation allows the use of efficient semidefinite programming solvers, which have polynomial worst-case complexity [31].

Definition 1 (SOS Polynomial). A multivariate polynomial $\lambda(x)$ is a *Sum-Of-Squares (SOS)* for $x \in \mathbb{R}^n$ if there exists some polynomials λ_i , $i = 1, \dots, r$, for some $r \in \mathbb{N}$, such that $\lambda(x) = \sum_{i=1}^r \lambda_i^2(x)$. If $\lambda(x)$ is an SOS, then $\lambda(x) \geq 0$ for all $x \in \mathbb{R}^n$. The set of all SOS polynomials is denoted by Λ .

Now, consider a basic closed semi-algebraic set $X = \{x \in \mathbb{R}^n \mid h_i(x) \geq 0 \ \forall i \in \{1, \dots, l\}\}$, which is defined as the intersection of l polynomial ($h_i(x)$) inequalities. Then, Proposition 1 allows one to enforce non-negativity on these semi-algebraic sets.

Proposition 1 (Putinar’s Certificate, [32]). Let $X \subset \mathbb{R}^n$ be a compact basic semi-algebraic set defined as $X = \{x \in \mathbb{R}^n \mid h_i(x) \geq 0 \ \forall i \in \{1, \dots, l\}\}$, where $h_i(x)$ is a polynomial. Then, polynomial $\gamma(x)$ is non-negative on X if, for some $\lambda_0(x), \lambda_i(x) \in \Lambda$, $\gamma(x) = \lambda_0(x) + \sum_{i=1}^l \lambda_i(x)h_i(x)$.

Corollary 1. Let $\gamma(x)$ be a non-negative polynomial on $X = \{x \in \mathbb{R}^n \mid h_i(x) \geq 0 \ \forall i \in \{1, \dots, l\}\}$, and $h(x)$ be an l -dimensional vector of polynomials with $h_i(x)$ as its i -th dimension for all $i \in \{1, \dots, l\}$. Further, let \mathcal{L} be an l -dimensional vector of SOS polynomials, i.e., the i -th element of \mathcal{L} is $\lambda_i(x) \in \Lambda$. Then, it holds that $\gamma(x) - \mathcal{L}^T h(x) \in \Lambda$.

4 Barrier Functions for Neural Network Dynamical Models

In this section, we introduce a formulation for synthesizing a barrier function that guarantees safety of System (1). Our approach relies on the local convex relaxations of f^w , which we use to formulate an SOS optimization problem that generates a valid barrier function for System (1).

4.1 Local Convex Relaxation of NNDMs

Our approach uses a convex relaxation of f^w . Specifically, we utilize the recent relaxation results for NNs [19] to compute piece-wise linear functions that under- and over-approximate f^w . The advantage of this method is that it is computationally efficient and produces tight bounds for small neighborhoods. To this end, we first partition X_s to a finite set of regions $Q = \{q_1, \dots, q_{|Q|}\}$, where $q_i \subseteq X_s$ for all $i \in \{1, \dots, |Q|\}$ is a basic (closed) semi-algebraic set. Such a decomposition can be obtained using, e.g., a grid or half-spaces. Then, for every $q \in Q$, we compute linear bounds

$$\underline{f}_q(x) = \underline{A}_q x + \underline{b}_q, \quad \overline{f}_q(x) = \overline{A}_q x + \overline{b}_q \quad \text{such that} \quad \forall x \in q, \quad \underline{f}_q(x) \leq f^w(x) \leq \overline{f}_q(x). \quad (6)$$

The above linear functions can be produced in several ways. One method is to forward propagate the bounds in the input domain of $f^w(x)$ using Interval Bound Propagation (IBP) based approaches [33, 34]. These approaches are efficient but generally lead to loose approximations. Another method is Linear Relaxation based Perturbation Analysis (LiRPA) algorithms, which perform a symbolic back propagation followed by a forward evaluation of the bounds [35, 36, 19]. Such LiRPA-based algorithms produce tighter bounds but can be slow. In our implementation, we use the off-the-shelf toolbox [36] to compute $\overline{f}_q(x)$ and $\underline{f}_q(x)$ in (6) for its trade-off between speed and accuracy.

4.2 Barrier Function (Certificate) Synthesis

Recall that a valid barrier function $B(x)$ must satisfy Conditions (4b)-(4d). With the above local linear bounds for f^w , Condition (4d) can be redefined over the partitioned regions in Q . That is, Condition (4d) can be replaced with the following constraints: for each $q \in Q$,

$$E[B(f_q^w(x) + \mathbf{v}) \mid x] \leq B(x)/\alpha + \beta \quad \text{and} \quad \underline{f}_q(x) \leq f_q^w(x) \leq \overline{f}_q(x) \quad \forall x \in q. \quad (7)$$

In this formulation, $f_q^w(x)$ is a (free) variable that is bounded by two linear functions, avoiding the non-convexity of $f_q^w(x)$. Consequently, an efficient evaluation of the constraint becomes feasible.

Remark 4. Note that there are in fact three constraints in (7) (one super-martingale condition on B and two bounds on $f_q^w(x)$). If they are treated separately, it leads to a conservative barrier function because each constraint needs to hold for all $x \in q$ separately. A less conservative approach is to pose all constraints for the same x at the same time. In Theorem 1, we show how this can be achieved.

As commonly practiced in the literature, e.g., [15, 8, 37], we restrict our search for a $B(x)$ to the class of polynomial functions. Then, the degree of the polynomial becomes a design parameter. In the following lemma, we show that the degree of the polynomial must be at least 2 for the polynomial to be a valid candidate barrier function for System (1). That is, there does not exist a linear function satisfying Conditions (4b)-(4d) for $\eta < 1$, which implies that the lower bound in (5) is trivially 0.

Lemma 1. For $k \in \mathbb{R}^n$ and $c \in \mathbb{R}$, consider linear function $B(x) = k^T x + c$. Then, $B(x)$ satisfies Conditions (4b)-(4d) iff $k = 0$ and $c = 1$.

Proof. There are two cases to consider: (i) $k = 0$: in this case $B(x) = c$, which satisfies Conditions (4b)-(4d) iff $c = \eta = 1$. (ii) $k \neq 0$: in this case, due to the linearity of $B(x)$, there always exists $x' \in \mathbb{R}^n$ such that $B(x') < 0$, violating Condition (4a). \square

Having established that the polynomial degree must be at least 2, we further restrict $B(x)$ to SOS polynomials. Theorem 1 shows a formulation of the barrier function synthesis problem as an SOS program, which can be solved in polynomial time. In particular, the theorem shows how to formulate Conditions (4b)-(4c) and (7) as SOS constraints.

Theorem 1 (NNDM Barrier Certificate). *Consider SOS polynomial function $B(x)$, and safe set $X_s = \{x \in \mathbb{R}^n \mid h_s(x) \geq 0\}$, initial set $X_0 = \{x \in \mathbb{R}^n \mid h_0(x) \geq 0\}$, unsafe set $X_u = \mathbb{R}^n \setminus X_s = \{x \in \mathbb{R}^n \mid h_u(x) \geq 0\}$, and partition region $q = \{x \in \mathbb{R}^n \mid h_q(x) \geq 0\}$ for all $q \in Q$. Let $\mathcal{L}_s(x)$, $\mathcal{L}_0(x)$ and $\mathcal{L}_u(x)$ be vectors of SOS polynomials with the same dimensions as h_s , h_0 , and h_u , respectively. Likewise, let $\mathcal{L}_{q,x}(x)$ and $\mathcal{L}_{q,y}(x)$ be vectors of SOS polynomials with the same dimension as h_q . Then, a stochastic barrier certificate $B(x)$ for System (1) with time horizon $N \in \mathbb{N}_{\geq 0}$ can be obtained by solving the following SOS optimization problem for $\eta, \beta \in [0, 1]$:*

$$\min_{\beta, \eta} \quad \eta + \beta N \quad \text{subject to:}$$

$$B(x) \in \Lambda, \tag{8a}$$

$$-B(x) - \mathcal{L}_0^T(x)h_0(x) + \eta \in \Lambda, \tag{8b}$$

$$B(x) - \mathcal{L}_u^T(x)h_u(x) - 1 \in \Lambda, \tag{8c}$$

$$E[B(y+v) \mid x] \leq B(x)/\alpha + \beta - \mathcal{L}_{q,x}^T(x)h_q(x) - \mathcal{L}_{q,y}^T(x)(\bar{f}_q(x) - y)(y - \underline{f}_q(x)) \in \Lambda \quad \forall q \in Q \tag{8d}$$

which guarantees safety probability $P_s(X_s, X_0, N) \geq 1 - (\eta + \beta N)$.

Proof. It suffices to show that if B satisfies Constraints (8a)-(8d), then Conditions (4a)-(4d) are satisfied. As Constraint (8a) guarantees that B is a SOS polynomial, hence non-negative by definition, Condition (4a) holds. By Corollary 1 it holds that if Constraints (8b)-(8c) hold, then B is respectively smaller than η in X_0 and greater than 1 in X_u . What is left to show is that Constraint (8d) guarantees the satisfaction of Condition (4d). This can be done as follows. For every region $q \in Q$, the expectation term in Condition (4d) can be expressed as $E[B(y+v) \mid x]$, where y is bounded by under-approximation $\underline{f}_q(x)$ and over-approximation $\bar{f}_q(x)$ of $f^w(x)$ in System (1) for all $x \in q$. Then by Corollary 1, Constraint (8d) is obtained for each q . Note that $B(x)$ is a polynomial, so if $E[B(y+v) \mid x]$ is also a polynomial, the condition is a valid SOS constraint. Given that $y+v$ is linear, $E[B(y+v) \mid x]$ is a sum of monomials in terms of y and expectation moments $\mathbb{E}[v^d]$, where $d \geq 0$. Since, random variable v has a normal distribution, $\mathbb{E}[v^d]$ is constant. Therefore, $E[B(y+v) \mid x]$ is a polynomial only in terms of (components of) y . \square

Remark 5. We note that Condition (8d) uses linear equations in (6) to bound $f^w(x)$ for all $x \in q$. Removing the dependence on x , by replacing the equations for $\bar{f}_q(x)$ and $\underline{f}_q(x)$ with their extreme values in region q , relaxes the optimization problem and results in a speed-up. It is however an additional over-approximation, and hence the obtained safety probability bound is strictly smaller than the one generated by using the actual linear equations for $\bar{f}_q(x)$ and $\underline{f}_q(x)$. This is the classical “efficiency versus accuracy” trade-off. In our implementation, we compare the two approaches.

5 Minimally-invasive Barrier Controller Synthesis

Here, we focus on Problem 2. The assumption is that a barrier function $B(x)$ is synthesized for System (1) via Theorem 1, which has a safety probability that is lower than threshold δ_s . Hence, our goal is to design a feedback controller for System (3) that guarantees safety. Ideally, this controller is minimal in the interruptions it causes to the system evolution. Below, we first provide a definition for a minimally-invasive controller, and then show how it can be synthesized.

Recall that a feedback controller $\pi : \mathbb{R}^n \rightarrow U$ is a function that assigns a control value to each state. Let $X_\pi \subseteq X_s$ be the set of states, to which π assigns non-zero control values, i.e., $\pi(x) \neq 0$ for all $x \in X_\pi$. Further, we denote by $V(X)$ the volume of set $X \subset \mathbb{R}^n$. Then, we say a feedback controller π is *minimally-invasive* if it minimizes $V(X_\pi)$. Moreover, we say π is ϵ -*minimally-invasive* if $V(X_\pi) - \min_{\pi'} V(X_{\pi'}) \leq \epsilon$. In this work, we seek ϵ -*minimally-invasive* controller with an arbitrary small ϵ . To this end, we make the observation that if the discretization of X_s discussed in Section 4.1

is uniform, $V(X_\pi)$ for a given π is directly proportional to the number of discrete regions in Q to which π applies a non-zero control. We denote by Q_π the set of such regions. Then, a feedback controller π that minimizes $|Q_\pi|$ is ϵ -minimally-invasive, and as the discretization becomes finer, ϵ monotonically approaches zero. Therefore, given barrier function $B(x)$, our first goal is to identify the minimal number of regions in Q that require a non-zero controller to guarantee safety. Recall that, given $B(x)$, we require the safety probability to be $1 - (\eta + \beta N) \geq \delta_s$. While η is related to the value of $B(x)$ in the initial set, β is a compensation needed to turn a sub-martingale inequality to a super-martingale inequality (Condition (8d) or (4d)). We can compute this compensation for each region $q \in Q$ by evaluating Condition (8d) or (4d). Let β_q denote the computed compensation term for region q . Then, region q requires a non-zero controller if $\beta_q > (1 - \delta_s - \eta)/N$.

We now turn our attention to designing a controller that reduces β_q . In our approach, we tap directly into the convex nature of the SOS polynomial $B(x)$ (SOS-convex). Lemma 2 shows that a controller that drives System (3) to a point closest to the minimum point of $B(x)$, also robustly minimizes β_q .

Lemma 2. *Given $B(x)$, let $x^* = \arg \min_x B(x)$, $x' = f^w(x) + gu + v$ as in System (3), and $\beta_q \geq E[B(x') \mid x] - B(x)$ for all x in region $q \subseteq X_s$. Then, the controller that minimizes $\|\tilde{x}' - x^*\|_1$, where $\tilde{x}' = f^w(x) + gu$, also robustly minimizes β_q , i.e., minimizes an upper bound of β_q .*

Proof. Given that B is a polynomial and x' is affine in both u and v , we can write $E[B(x') \mid x] = B(E[x' \mid x]) + \xi$, where ξ , called Jensen's gap [38], is a non-negative polynomial of x , u , and moments $E[v^d]$, where $2 \leq d \leq m$ is an even integer. This polynomial can always be upper bounded by a constant $\bar{\xi} \geq 0$ for bounded x and u . Then, with $\tilde{x}' = E[x']$, the min β_q is upper bounded by

$$\min_u \beta_q \leq \min_u \max_{x \in q} (B(\tilde{x}' \mid x) - B(x) + \bar{\xi}) \leq \min_u \max_{x \in q} B(\tilde{x}' \mid x) - \min_{x \in q} B(x) + \bar{\xi}.$$

The second inequality holds because B is a non-negative function resulting from a SOS optimization, and is thus SOS-convex [39]. Since $B(\tilde{x}')$ monotonically decreases as $\tilde{x}' \rightarrow x^*$, $\max_{x \in q} B(\tilde{x}' \mid x)$ is minimized by $\arg \min_u \|f^w(x) + gu - x^*\|_1 \forall x \in q$. \square

We note that, in the proof of Lemma 2, the moments $E[v^d]$ appear in every monomial of polynomial ξ (Jensen's gap). Hence, for v with variance less than 1, Jensen's gap is very small and vanishes as the variance becomes smaller, making the controller in the lemma optimal. Furthermore, even though Lemma 2 uses L_1 norm for $\|\tilde{x}' - x^*\|_1$, the statement also holds for L_2 and L_∞ norms. We specifically use L_1 norm to be able to compute the controller via an LP as stated in Theorem 2.

Theorem 2 (Controller Synthesis). *Consider convex barrier function $B(x)$ and its minimum argument x^* as specified in Lemma 2, and linear bounds $\underline{f}_q(x)$ and $\bar{f}_q(x)$ for $f^w(x)$ in region $q \subseteq \mathbb{R}^n$ as in (6). A controller that robustly minimizes β_q for System (3) is the solution to the following LP optimization problem, where $\theta = (\theta_1, \theta_2, \dots, \theta_n) \in \mathbb{R}_{\geq 0}^n$, and the vector inequality relations are element-wise:*

$$\begin{aligned} \min_{\theta_i, z', z'', u} \quad & \sum_{i=1}^n \theta_i \quad \text{subject to:} \\ & y - x^* \leq \theta \quad (10a) \quad y \geq \underline{f}_q(z) + gu \quad (10d) \\ & x^* - y \leq \theta \quad (10b) \quad y \leq \bar{f}_q(z) + gu \quad (10e) \\ & z = z' - z'' \quad (10c) \quad z', z'' \geq 0, z \in q, u \in U \quad (10f) \end{aligned}$$

Proof. By Lemma 2 it holds that to robustly minimize β_q , it suffices to minimize $\|\tilde{x}' - x^*\|_1$. This norm is the sum of n absolute values, each of which can be set to θ_i with linear Constraints (10a) and (10b). Hence, the minimization of $\|\tilde{x}' - x^*\|_1$ is equivalent to minimization of $\sum_{i=1}^n \theta_i$ subject to (10a) and (10b). The bounds on the dynamics of System (3) can be expressed as linear Conditions (10d) and (10e), each of which has to hold for all $z \in q$, i.e., z is a free variable. To turn the optimization into an LP, z is expressed as the difference of two non-negative decision variables z' and z'' in Constraint (10c). \square

Remark 6. *Note that the controller obtained via the LP is a vector of scalars for each region q . This leads to a feedback controller π over the regions $q \in Q$. It is possible to express u as SOS polynomials, which would be a feedback controller over x . That could potentially provide a tighter bound for β_q at the cost of extra computation since SOS optimization is more expensive than LP.*

5.1 Control Synthesis Algorithm

Our framework for computing a barrier certificate as well as minimally-invasive controllers for NNDMs is outlined in Algorithm 1. First, the safe set X_s is uniformly partitioned into a finite set of regions $|Q|$, and bounds of f^w are computed as piece-wise linear functions per Section 4.1. Then, for a given polynomial degree $m \geq 2$, a barrier certificate along with its corresponding safety probability bound are computed in accordance with Theorem 1. If this probability is greater than or equal to δ_s , the NNDM is certified, and the algorithm terminates. Otherwise, it iteratively searches for ϵ -minimally-invasive controllers. In each iteration, upper bound $\bar{\eta}$ is set on η (initially with its largest possible value $1 - \delta_s$ and then reduced by $\Delta\eta > 0$), and a new barrier function is computed with this bound, where the objective function is minimization of β to ensure ϵ -minimally-invasive controllers. Then, for each $q \in Q$, β_q is checked against the threshold. If exceeding, a controller is computed for q in accordance with Theorem 2. This process repeats until a satisfactory P_s is obtained or $\bar{\eta} < 0$.

We highlight two important properties of this algorithm: it clearly terminates in finite time, and if $P_s \geq \delta_s$, the synthesized controller is correct-by-construction.

Algorithm 1: NNDM Controller Synthesis

Input : NN f^w , initial set X_0 , safe set X_s , noise covariance R , polynomial degree m , threshold δ_s , and step size $\Delta\eta$
Output : feedback controller π , and safety probability bound P_s

```

1  $Q, \underline{f}_q, \bar{f}_q \leftarrow \text{PARTITIONANDCOMPUTEBOUNDS}(X_s, f^w), \quad k \leftarrow 0$ 
2  $\eta, \beta, B(x) \leftarrow \text{COMPUTE BARRIER CERTIFICATE}(Q, \underline{f}_q, \bar{f}_q, R, m)$  // Theorem 1
3 while  $P_s < \delta_s$  and  $\bar{\eta} > 0$  do
4    $\bar{\eta} \leftarrow 1 - (\delta_s - k\Delta\eta), \quad k \leftarrow k + 1$  // set upper bound on  $\eta$ 
5    $\eta, \beta, B(x) \leftarrow \text{COMPUTE BARRIER CERTIFICATE}(Q, \underline{f}_q, \bar{f}_q, R, m, \bar{\eta})$  // Theorem 1
6   for  $q \in Q$  do
7      $\pi \leftarrow (q, 0)$ 
8     if  $\beta_q > (1 - \delta_s - \eta)/N$  then
9        $\pi \leftarrow (q, u_q) \leftarrow \text{COMPUTE CONTROL}(\arg \min B(x), q, \underline{f}_q, \bar{f}_q, U)$  // Theorem 2
10       $\beta_q \leftarrow \text{UPDATE BETA}(B(x), u_q)$  // evaluate Condition (8d)
11    $P_s \leftarrow 1 - (\eta + N \max_{q \in Q} \beta_q)$ 
12 return  $\pi, P_s$ 
```

6 Case Studies

We demonstrate the efficacy of our framework on several case studies. We first show that our verification method is able to produce non-trivial safety guarantees for NNDMs trained using imitation learning techniques [40] from data gathered by rolling out an RL agent trained with state-of-the-art RL techniques [41]. We then show that our control approach significantly increases the safety probability.

Models We trained the *Pendulum* (2D), *Cartpole* (4D), and *Acrobot* (6D) agents from the OpenAI gym environment, as well as 4D and 5D *Husky robot* models. For the OpenAI models, we collected input-output states of the system under an expert controller, either as a look-up table or an NN controller. We picked the best controller available for the agents from the OpenAI Leaderboard [41]. The Husky models were trained to move from one point to another while staying within a lane. We initially trained a NNDM along with an NN controller on the trajectory data generated from PyBullet (physics simulator [42]) as outlined in [9]. We then used these NNs to generate input-output data and trained closed-loop NNDMs as specified above. In total, we trained 10 fully-connected multi-layer perceptron NNDM architectures with up to 5 hidden layers and 512 neurons per layer, each with ReLU activation function. The dimensionality and architecture information is provided in Table 1.

The state space of the Pendulum consists of the pole angle θ and angular velocity $\dot{\theta}$, with the safe set defined as $[-\pi/15, \pi/15] \times [-1, 1]$, and the initial set as $\theta_0 \in [-\pi/36, \pi/36]$. For the Cartpole, the state space consists of the cart position x , velocity \dot{x} , pole angle θ , and angular velocity $\dot{\theta}$. The safe sets for cart position are defined as $x \in [-1, 1]$ and $\theta \in [-\pi/15, \pi/15]$, with the initial set $\theta_0 \in [-\pi/36, \pi/36]$. For the 4D Husky, the states are position x and y , orientation θ , and linear velocity v . The task of the controller is to keep the robot within a lane, and hence the safe set is $y \in [-1, 1]$, and the initial set is defined as any position (x, y) that is within a radius of 0.1 from the

Table 1: Benchmark results for barrier certificate and control synthesis on various NNDMs. Threshold $\delta_s = 0.95$ was used for the minimally-invasive control synthesis. Architecture $h \times [r]$ denotes a NNDM with h hidden layers, each with r neurons. n is the dimensionality of the system.

Model	n	$h \times [r]$	$ Q $	Verification						Control					
				Interval Bounds			Linear Bounds			Interval Bounds			Linear Bounds		
				β	P_s	Time (min)	β	P_s	Time (min)	β	P_s	Time (min)	β	P_s	Time (min)
Pendulum	2	1 x [64]	120	0.540	0.459	0.09	0.002	0.997	0.09	10^{-6}	0.999	0.04	-	-	-
			240	0.444	0.555	0.13	0.002	0.997	0.14	10^{-6}	0.999	0.11	-	-	-
			480	0.155	0.844	0.38	0.003	0.997	0.43	10^{-6}	0.999	0.36	-	-	-
		2 x [64]	120	0.575	0.424	0.05	0.191	0.785	0.07	10^{-6}	0.999	0.04	10^{-6}	0.999	0.05
			240	0.471	0.526	0.14	0.153	0.844	0.15	10^{-6}	0.998	0.11	10^{-6}	0.998	0.13
			480	0.196	0.801	0.39	0.075	0.922	0.47	10^{-6}	0.997	0.32	10^{-6}	0.997	0.34
	3	3 x [64]	120	0.689	0.305	0.05	0.384	0.603	0.07	10^{-6}	0.994	0.03	10^{-6}	0.986	0.04
			240	0.555	0.439	0.14	0.288	0.708	0.15	10^{-6}	0.995	0.11	10^{-6}	0.995	0.13
			480	0.357	0.636	0.39	0.208	0.790	0.45	10^{-6}	0.994	0.36	10^{-6}	0.998	0.46
		5 x [64]	480	0.878	0.027	0.42	0.735	0.172	0.46	10^{-6}	0.901	0.37	10^{-6}	0.951	0.40
			960	0.635	0.270	1.45	0.603	0.302	1.56	10^{-6}	0.905	1.37	10^{-6}	0.951	1.59
			1920	0.449	0.447	5.96	0.421	0.504	6.61	10^{-6}	0.905	5.29	10^{-6}	0.951	5.36
Cartpole	4	1 x [128]	960	1.00	0.00	17.31	0.623	0.376	17.99	10^{-6}	0.874	12.38	10^{-6}	0.998	13.35
			1920	1.00	0.00	59.98	0.414	0.578	65.15	10^{-6}	0.899	31.21	10^{-6}	0.992	35.09
			3840	0.794	0.195	215.23	0.382	0.602	234.79	10^{-6}	0.980	156.86	10^{-6}	0.984	160.99
		2 x [128]	960	1.00	0.00	17.63	0.811	0.181	19.85	10^{-6}	0.814	12.08	10^{-6}	0.993	13.30
			1920	1.00	0.00	35.50	0.779	0.216	36.89	10^{-6}	0.847	32.19	10^{-6}	0.997	36.89
			3840	0.877	0.102	230.50	0.664	0.333	239.21	10^{-6}	0.979	150.31	10^{-6}	0.997	162.57
Husky	4	1 x [256]	900	0.672	0.200	15.56	0.431	0.367	16.65	10^{-6}	0.872	11.46	10^{-6}	0.951	11.81
			1800	0.667	0.211	53.34	0.425	0.382	53.56	10^{-6}	0.878	33.15	10^{-6}	0.951	33.73
			2250	0.645	0.288	68.41	0.367	0.495	81.32	10^{-6}	0.933	42.74	10^{-6}	0.951	46.49
		2 x [256]	4800	0.622	0.331	307.61	0.347	0.539	345.29	10^{-6}	0.951	299.98	10^{-6}	0.953	304.66
			1800	1.00	0.00	64.56	0.544	0.011	74.69	10^{-6}	0.756	31.33	10^{-6}	0.800	35.22
			2250	1.00	0.00	69.57	0.502	0.222	74.83	10^{-6}	0.847	50.07	10^{-6}	0.951	51.76
Husky	5	1 x [512]	4800	0.845	0.062	369.90	0.415	0.384	406.70	10^{-6}	0.907	297.57	10^{-6}	0.951	306.41
			432	1.00	0.00	10.33	1.00	0.00	11.64	10^{-1}	0.749	7.69	10^{-6}	0.851	8.34
			1080	1.00	0.00	51.59	1.00	0.00	57.65	10^{-3}	0.829	50.09	10^{-6}	0.950	52.08
Acrobot	6	1 x [512]	1728	1.00	0.00	169.87	1.00	0.00	171.23	10^{-3}	0.945	161.43	10^{-6}	0.951	163.80
			144	1.00	0.00	11.53	1.00	0.00	12.37	10^{-6}	0.951	4.01	10^{-6}	0.951	4.45
			288	1.00	0.00	24.59	0.872	0.08	26.80	10^{-6}	0.951	11.34	10^{-6}	0.951	12.06

origin. For the 5D Husky, the additional state over the 4D model is the angular velocity ω ; the task, the safe set, and the initial set remain the same. Finally, for the Acrobot, the state space consists of the cosines and sines of θ_1 and θ_2 , and angular velocities $\dot{\theta}_1$ and $\dot{\theta}_2$. Here θ_1 and θ_2 are the pole angle of the first link and the angle of the second link relative to the first link, respectively. The task is for the tip of the second link to reach a height of at least $y = 1$, with a safety constraint to never reach beyond $y = 1.2$. Thus, the safe set is defined as $\sin(\theta_1) \in [-0.6, 0.6]$ and $\sin(\theta_2) \in [-0.6, 0.6]$, and the initial set is any point within a radius of 0.1 around the origin in the first 4 dimensions.

Implementation and Experimental Setup: We implemented our algorithms in Python and Julia (code available in [43]). For collecting data and training, we used the TensorFlow framework [44]. To compute the linear approximations of the NNDMs, we utilized α -CROWN [36]. For the optimization, we used Julia's *SumOfSquares.jl* package [45, 46]. The optimizations are all performed single-threaded on a computer with 3.9 GHz 8-Core CPU and 64 GB of memory.

Benchmarks: To the best of our knowledge, there is no other work on safety verification of NNDMs, against which we can compare. Hence as a baseline, we compare our approach based on linear under and over approximation of the NNDM against interval bounding approaches cf. Remark 5. The interval bounding approach results in a relaxed optimization problem at the cost of more conservative safety probabilities. The results are shown in Table 1. The computation times indicate the time to synthesize the barrier and the controller using Theorems 1 and 2, respectively. The barrier degree is 4 for all the case studies. Below, we provide a brief discussion on the results. For more in-depth discussions and details on the discretization and hyperparameters, see Appendix A.

Verification: As expected, the safety probability always increases with $|Q|$ (finer partitions), since the linear and interval bounds for f^w become more accurate. This behavior is encountered in all the systems and architectures, regardless of the number of hidden layers or neurons per layer. However, it is also observed that this trend of finer discretizations and increased safety probability consistently comes at the cost of an increased computation time. This is due to the fact that the number of partitions directly dictate the number of constraints in the optimization problems. Note that the probability of safety using interval bounds is strictly worse than linear approximations for all the experiments. Using either linear or interval bounds, we are able to compute non-trivial probability of safety for all the case-studies and observe the discretization vs accuracy trend. Take for instance, the 1-layer Cartpole model, where an increase in $|Q|$ from 960 to 3840 causes an increase in P_s from

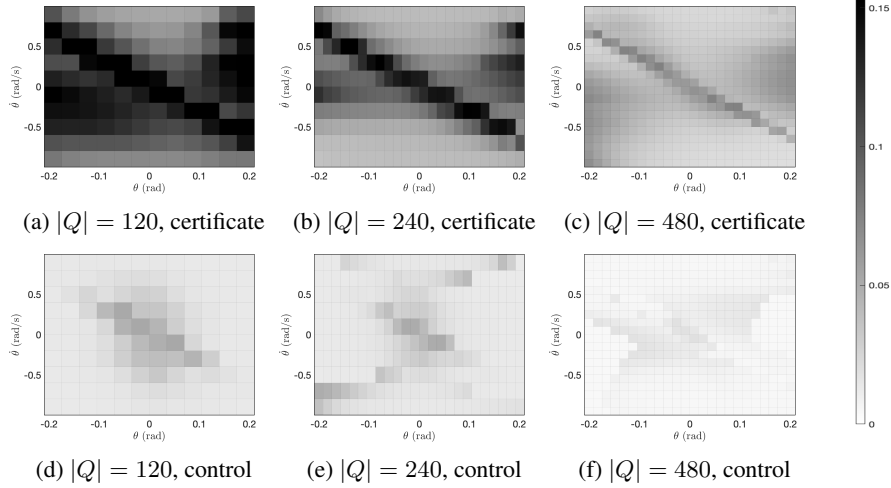


Figure 1: Comparison of β_q values for the Pendulum NNDM with 2 layers and 64 neurons per layer before and after applying the controller for various $|Q|$. Shade of gray correspond to the values of β_q .

0.375 to 0.602, at the expense of an increased computation time of more than 12 times. This behavior is also true for the 4D Husky model, where increasing $|Q|$ from 1800 to 4800 for the 2-layer model, increases P_s from 0.011 to 0.384 at the price of a more than 5-fold increase in the computation time.

Control Synthesis: When the certification probability is below $\delta_s = 0.95$, the control strategy is utilized to increase the probability of safety. Using interval bounds, controllers had to be synthesized for all case-studies, which illustrates the looseness of the bounds. In fact, in several case studies, the controller was not able to meet the desired threshold. For the linear bounds, observe that for all except two NNDMs, whose $P_s < \delta_s$, the controller synthesis algorithm was able to produce $P_s \geq \delta_s$, showing the effectiveness of our control method. The first exception is for the 4D Husky model with 2-hidden layers and $|Q| = 1800$, where the controller increases P_s from 0.011 to 0.800 (73-fold increase) yet cannot meet the 0.95 threshold. Similarly, for the 1-layer 5D Husky model with $|Q| = 432$, the controller increases P_s from 0.00 to 0.851, but the 0.95 threshold cannot be reached. Nonetheless, for all the linear bound cases, the controller reduces β to 10^{-6} .

Figure 1 illustrates the minimally-invasive aspect of the controllers. It shows the β_q values for the Pendulum NNDM with 2 layers before and after the application of the controllers with three different sizes of $|Q|$. For $|Q| = 120$, all the regions require controllers, but for $|Q| = 240$ and 480, respectively, only 69.2% and 23.75% of the regions require controllers; hence, the minimally-invasive controller focuses specifically on those regions and does not affect those with already-small β_q .

7 Conclusion

In this work, we introduced a methodology for providing safety guarantees for NNDMs using stochastic barrier functions. We showed that the problem of finding a stochastic barrier function for a NNDM can be relaxed to an SOS optimization problem. Furthermore, we derived a novel framework for synthesis of an affine controller with the goal of maximizing the safety probability in a minimally-invasive manner. Experiments showcase that, along with a minimally-invasive controller, we can guarantee safety for various standard reinforcement learning problems.

A bottleneck to our approach is the discretization step, which is required to obtain piece-wise linear under- and over-approximations of the neural network, and can be expensive for higher dimensional spaces. Future directions should focus on mitigating this curse of dimensionality.

Acknowledgments and Disclosure of Funding

This work was supported in part by the NSF grant 2039062 and NASA COLDTech Program under grant #80NSSC21K1031.

References

- [1] Christel Baier and Joost-Pieter Katoen. *Principles of model checking*. MIT Press, 2008.
- [2] Morteza Lahijanian, Sean B Andersson, and Calin Belta. Temporal logic motion planning and control with probabilistic satisfaction guarantees. *IEEE Transactions on Robotics*, 28(2):396–409, 2011.
- [3] Luca Laurenti, Morteza Lahijanian, Alessandro Abate, Luca Cardelli, and Marta Kwiatkowska. Formal and efficient synthesis for continuous-time linear stochastic hybrid processes. *IEEE Transactions on Automatic Control*, 2020.
- [4] Calin Belta and Sadra Sadraddini. Formal methods for control synthesis: An optimization perspective. *Annual Review of Control, Robotics, and Autonomous Systems*, 2:115–140, 2019.
- [5] Maziar Raissi, Paris Perdikaris, and George E Karniadakis. Physics-informed neural networks: A deep learning framework for solving forward and inverse problems involving nonlinear partial differential equations. *Journal of Computational physics*, 378:686–707, 2019.
- [6] John Cristian Borges Gamboa. Deep learning for time-series analysis. *arXiv preprint arXiv:1701.01887*, 2017.
- [7] Stephen Prajna, Ali Jadbabaie, and George J Pappas. A framework for worst-case and stochastic safety verification using barrier certificates. *IEEE Transactions on Automatic Control*, 52(8):1415–1428, 2007.
- [8] Cesar Santoyo, Maxence Dutreix, and Samuel Coogan. A barrier function approach to finite-time stochastic system verification and control. *Automatica*, 125:109439, 2021.
- [9] Anusha Nagabandi, Gregory Kahn, Ronald S Fearing, and Sergey Levine. Neural network dynamics for model-based deep reinforcement learning with model-free fine-tuning. In *2018 IEEE International Conference on Robotics and Automation (ICRA)*, pages 4063–4069. IEEE, 2017.
- [10] Ricky TQ Chen, Yulia Rubanova, Jesse Bettencourt, and David K Duvenaud. Neural ordinary differential equations. *Advances in neural information processing systems*, 31, 2018.
- [11] Kurtland Chua, Roberto Calandra, Rowan McAllister, and Sergey Levine. Deep reinforcement learning in a handful of trials using probabilistic dynamics models. In *Advances in Neural Information Processing Systems*, pages 4754–4765, 2018.
- [12] Keene Chin, Tess Hellebrekers, and Carmel Majidi. Machine learning for soft robotic sensing and control. *Advanced Intelligent Systems*, 2(6):1900171, 2020.
- [13] Aaron D. Ames, Samuel Coogan, Magnus Egerstedt, Gennaro Notomista, Koushil Sreenath, and Paulo Tabuada. Control barrier functions: Theory and applications. In *2019 18th European Control Conference (ECC)*, pages 3420–3431, 2019.
- [14] Stephen Prajna and Ali Jadbabaie. Safety verification of hybrid systems using barrier certificates. In *International Workshop on Hybrid Systems: Computation and Control*, pages 477–492. Springer, 2004.
- [15] Stephen Prajna, Ali Jadbabaie, and George J. Pappas. A framework for worst-case and stochastic safety verification using barrier certificates. *IEEE Transactions on Automatic Control*, 52(8):1415–1428, 2007.
- [16] Aaron D Ames, Jessy W Grizzle, and Paulo Tabuada. Control barrier function based quadratic programs with application to adaptive cruise control. In *53rd IEEE Conference on Decision and Control*, pages 6271–6278. IEEE, 2014.
- [17] Ian J. Goodfellow, Jonathon Shlens, and Christian Szegedy. Explaining and harnessing adversarial examples. *CoRR*, abs/1412.6572, 2015.

- [18] Guy Katz, Clark Barrett, David L Dill, Kyle Julian, and Mykel J Kochenderfer. Reluplex: An efficient SMT solver for verifying deep neural networks. In *International Conference on Computer Aided Verification*, pages 97–117. Springer, 2017.
- [19] Huan Zhang, Tsui-Wei Weng, Pin-Yu Chen, Cho-Jui Hsieh, and Luca Daniel. Efficient neural network robustness certification with general activation functions. *Advances in neural information processing systems*, 31, 2018.
- [20] Ruediger Ehlers. Formal verification of piece-wise linear feed-forward neural networks. In *International Symposium on Automated Technology for Verification and Analysis*, pages 269–286. Springer, 2017.
- [21] Mathias Lechner, Đorđe Žikelić, Krishnendu Chatterjee, and Thomas Henzinger. Infinite time horizon safety of bayesian neural networks. *Advances in Neural Information Processing Systems*, 34, 2021.
- [22] Sophie Gruenbacher, Ramin M. Hasani, Mathias Lechner, Jacek Cyranka, Scott A. Smolka, and Radu Grosu. On the verification of neural odes with stochastic guarantees. In *AAAI*, 2021.
- [23] Charles Dawson, Sicun Gao, and Chuchu Fan. Safe control with learned certificates: A survey of neural lyapunov, barrier, and contraction methods. *arXiv preprint arXiv:2202.11762*, 2022.
- [24] Matthew Wicker, Luca Laurenti, Andrea Patane, Nicola Paoletti, Alessandro Abate, and Marta Kwiatkowska. Certification of iterative predictions in bayesian neural networks. *Uncertainty in Artificial Intelligence (UAI)*, 2021.
- [25] Steven Adams, Morteza Lahijanian, and Luca Laurenti. Formal control synthesis for stochastic neural network dynamic models. *IEEE Control Systems Letters*, 2022.
- [26] Tianhao Wei and Changliu Liu. Safe control with neural network dynamic models. In *Learning for Dynamics and Control Conference*, pages 739–750. PMLR, 2022.
- [27] Dimitris Bertsekas and Steven Shreve. *Stochastic optimal control: the discrete-time case*. Athena Scientific, 2004.
- [28] Murray Marshall. *Positive polynomials and sums of squares*. American Mathematical Soc., 2008.
- [29] Harold J Kushner. Stochastic stability and control. Technical report, Brown Univ Providence RI, 1967.
- [30] Hilbert. Ueber die darstellung definiter formen als summen von formenquadraten. *Mathematische Annalen*, 32:342–350, 1888.
- [31] Lieven Vandenbergh and Stephen Boyd. Semidefinite programming. *SIAM review*, 38(1):49–95, 1996.
- [32] Gilbert Stengle. A nullstellensatz and a positivstellensatz in semialgebraic geometry. *Mathematische Annalen*, 207:87–98, 1974.
- [33] Shiqi Wang, Kexin Pei, Justin Whitehouse, Junfeng Yang, and Suman Jana. Efficient formal safety analysis of neural networks. In *Advances in Neural Information Processing Systems*, pages 6367–6377, 2018.
- [34] Shiqi Wang, Kexin Pei, Justin Whitehouse, Junfeng Yang, and Suman Jana. Formal security analysis of neural networks using symbolic intervals. In *27th USENIX Security Symposium (USENIX Security 18)*, pages 1599–1614, 2018.
- [35] Shiqi Wang, Huan Zhang, Kaidi Xu, Xue Lin, Suman Jana, Cho-Jui Hsieh, and J. Zico Kolter. Beta-crown: Efficient bound propagation with per-neuron split constraints for complete and incomplete neural network robustness verification. *Advances in Neural Information Processing Systems*, 34:29909–29921, 2021.

- [36] Kaidi Xu, Huan Zhang, Shiqi Wang, Yihan Wang, Suman Jana, Xue Lin, and Cho-Jui Hsieh. Fast and complete: Enabling complete neural network verification with rapid and massively parallel incomplete verifiers. *International Conference on Learning Representations*, 2020.
- [37] Jacob Steinhardt and Russ Tedrake. Finite-time regional verification of stochastic non-linear systems. *The International Journal of Robotics Research*, 31(7):901–923, 2012.
- [38] JG Liao and Arthur Berg. Sharpening jensen’s inequality. *The American Statistician*, 2018.
- [39] Amir Ali Ahmadi and Raphaël M. Jungers. Sos-convex lyapunov functions with applications to nonlinear switched systems. In *Proceedings of the IEEE Conference on Decision and Control*, 2013.
- [40] Steven L Brunton and J Nathan Kutz. *Data-driven science and engineering: Machine learning, dynamical systems, and control*. Cambridge University Press, 2022.
- [41] Gym leaderboard. <https://github.com/openai/gym/wiki/Leaderboard>.
- [42] Erwin Coumans and Yunfei Bai. Pybullet, a python module for physics simulation for games, robotics and machine learning. <http://pybullet.org>, 2016–2021.
- [43] Github code: NeuralNetControlBarrier. <https://github.com/aria-systems-group/NeuralNetControlBarrier>.
- [44] Martín Abadi, Ashish Agarwal, Paul Barham, Eugene Brevdo, Zhifeng Chen, Craig Citro, Greg S. Corrado, Andy Davis, Jeffrey Dean, Matthieu Devin, Sanjay Ghemawat, Ian Goodfellow, Andrew Harp, Geoffrey Irving, Michael Isard, Yangqing Jia, Rafal Jozefowicz, Lukasz Kaiser, Manjunath Kudlur, Josh Levenberg, Dandelion Mané, Rajat Monga, Sherry Moore, Derek Murray, Chris Olah, Mike Schuster, Jonathon Shlens, Benoit Steiner, Ilya Sutskever, Kunal Talwar, Paul Tucker, Vincent Vanhoucke, Vijay Vasudevan, Fernanda Viégas, Oriol Vinyals, Pete Warden, Martin Wattenberg, Martin Wicke, Yuan Yu, and Xiaoqiang Zheng. TensorFlow: Large-scale machine learning on heterogeneous systems, 2015. Software available from tensorflow.org.
- [45] Tillmann Weisser, Benoît Legat, Chris Coey, Lea Kapelevich, and Juan Pablo Vielma. Polynomial and moment optimization in julia and jump. In *JuliaCon*, 2019.
- [46] Benoît Legat, Chris Coey, Robin Deits, Joey Huchette, and Amelia Perry. Sum-of-squares optimization in Julia. In *The First Annual JuMP-dev Workshop*, 2017.
- [47] Husky urdf clearpath. <https://github.com/bulletphysics/bullet3/blob/master/data/husky/husky.urdf>.
- [48] Giuseppe Paolo, Jonas Gonzalez-Billandon, Albert Thomas, and Balázs Kégl. Guided safe shooting: model based reinforcement learning with safety constraints. *arXiv preprint arXiv:2206.09743*, 2022.

A Additional Discussions on the Experiments

In this section, we first delineate a more in-depth discussion and detailed description of the training process for the Pendulum and Cartpole NNDMs. We then showcase our experiments on two of the OpenAI agents by providing simulation results for both the certification and the control of the NNDMs. At last, a detailed description on the training process for the Husky and Acrobot is provided. Table 2 shows the partition width in each dimension for all the NNDMs.

A.1 Pendulum and Cartpole

We trained NNDMs with fixed number of epochs (300) and implemented an early stopping method to avoid over-fitting. The number of data points were increased from 5,000 to 50,000 as the depth of the NNDM increased for a fixed model, ranging from 1 layer to 5 layers. Figure 2 shows the vector fields of the pendulum NNDMs with various architectures.

Pendulum In this case-study, we trained a NNDM for a Pendulum agent which has fixed mass m and length l with actuator limits $u \in [-1, 1]$. We trained the NN under a given controller from [41] that tries to keep the pendulum upright. We modified the original OpenAI gym environment and directly learned the evolution of state variables θ and $\dot{\theta}$. We trained $f^w : \mathbb{R}^2 \rightarrow \mathbb{R}^2$ with one to five hidden layers with 64 neurons each. The NNDM is trained in region $\theta \in [-\pi, \pi]$ and $\dot{\theta} \in [-1, 1]$. The safe set is $\theta \in [-\frac{\pi}{15}, \frac{\pi}{15}]$ and $\dot{\theta} \in [-1, 1]$ and the initial set is $\theta \in [-\frac{\pi}{36}, \frac{\pi}{36}]$. The state space X is as mentioned in Table 3. We compute linear bounds for various discretization sizes as discussed in Section 4.1 and Table 2.

The dynamics of the system is

$$\dot{\theta}_{k+1} = \dot{\theta}_k + \frac{3g}{2l} \sin(\theta_k) \delta t^2 + \frac{3}{ml^2} u \delta t^2, \quad (11)$$

$$\theta_{k+1} = \theta_k + \dot{\theta}_{k+1} \delta t \quad (12)$$

For the Pendulum 1-layer NNDM models, we notice that the probability of safety is above δ_s even for coarser discretizations. In general, we observe that for a fixed model, the probability of safety

Table 2: Discretization parameters for each model of dimension n for various partitioning $|Q|$.

Model	n	$ Q $	Discretization					
Pendulum	2	120	θ		$\dot{\theta}$			
		240	0.01745329		0.1			
		480	0.00872664		0.1			
		960	0.00872664		0.05			
		1920	0.00436332		0.05			
Cartpole	4	960	x		\dot{x}	θ	$\dot{\theta}$	
		1920	0.2		0.125	0.01745329	0.125	
		3840	0.2		0.125	0.01745329	0.0625	
		3840	0.1		0.125	0.000872665	0.125	
Husky	4	900	x		y	θ	v	
		1800	0.2		0.2	0.01745329	0.2	
		2250	0.2		0.2	0.00872665	0.2	
		4800	0.2		0.2	0.01745329	0.1	
		4800	0.125		0.125	0.01745329	0.125	
Husky	5	432	x		\dot{x}	θ	$\dot{\theta}$	ω
		1080	0.2		0.2	0.01745329	0.2	0.2
		1728	0.2		0.1	0.01745329	0.2	0.2
		1728	0.2		0.2	0.01745329	0.125	0.125
Acrobot	6	144	$\cos(\theta_1)$	$\sin(\theta_1)$	$\cos(\theta_2)$	$\sin(\theta_2)$	$\dot{\theta}_1$	$\dot{\theta}_2$
		288	0.05	0.1	0.05	0.1	0.25	0.25
		288	0.05	0.05	0.05	0.1	0.25	0.25

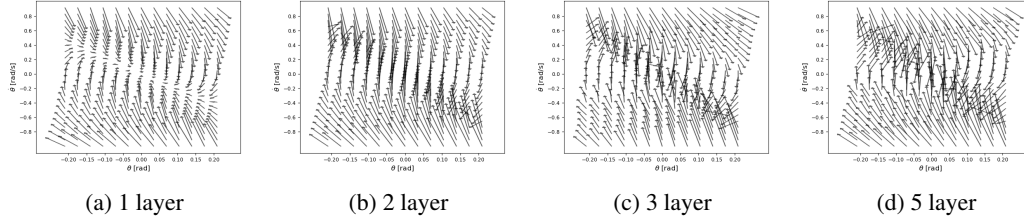


Figure 2: Vector fields of the NNDMs for the Pendulum agent with various architectures.

increases as the discretization becomes finer. For a fixed discretization, the general trend is a decrease in probability of safety as the model gets deeper (more hidden layers).

Figure 3 shows the evolution of the state variables with and without the controller π and the control evolution u under π for the 3-layer NNDM model. We observe that the NNDM without the controller has more oscillation while the system using the minimally invasive controller is more stable. In one simulation, we observed that the system's state comes close to unsafe region and the controller is successfully able to push the system to the safe set. We also note that the controller magnitude varies from 0.1 to -0.4 which is within its bounds of $[-1, 1]$.

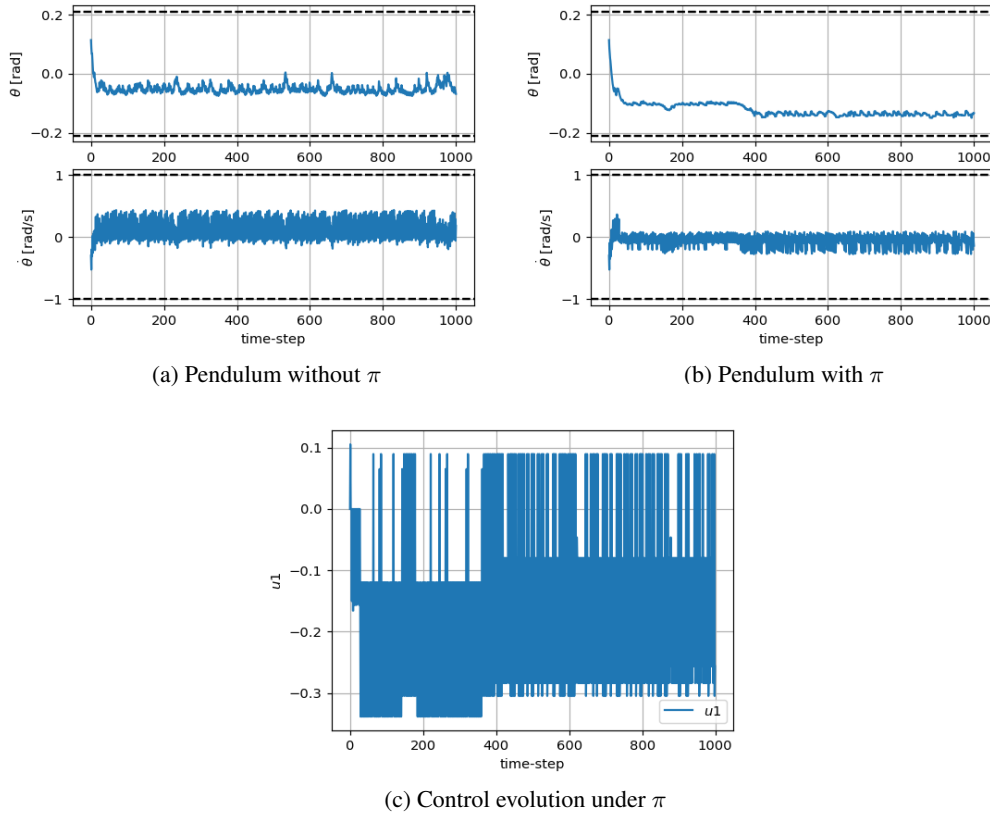


Figure 3: State evolution of the Pendulum 3 layer NNDM model for 1000 steps with and without safety feedback controller π . Blue line shows state evolution for the system starting at $\theta = 0.114$, and $\dot{\theta} = -0.3$. Black dotted line demarcates the safe space (X_s) for the system. The initial state corresponds to the partition (q) with the highest β value.

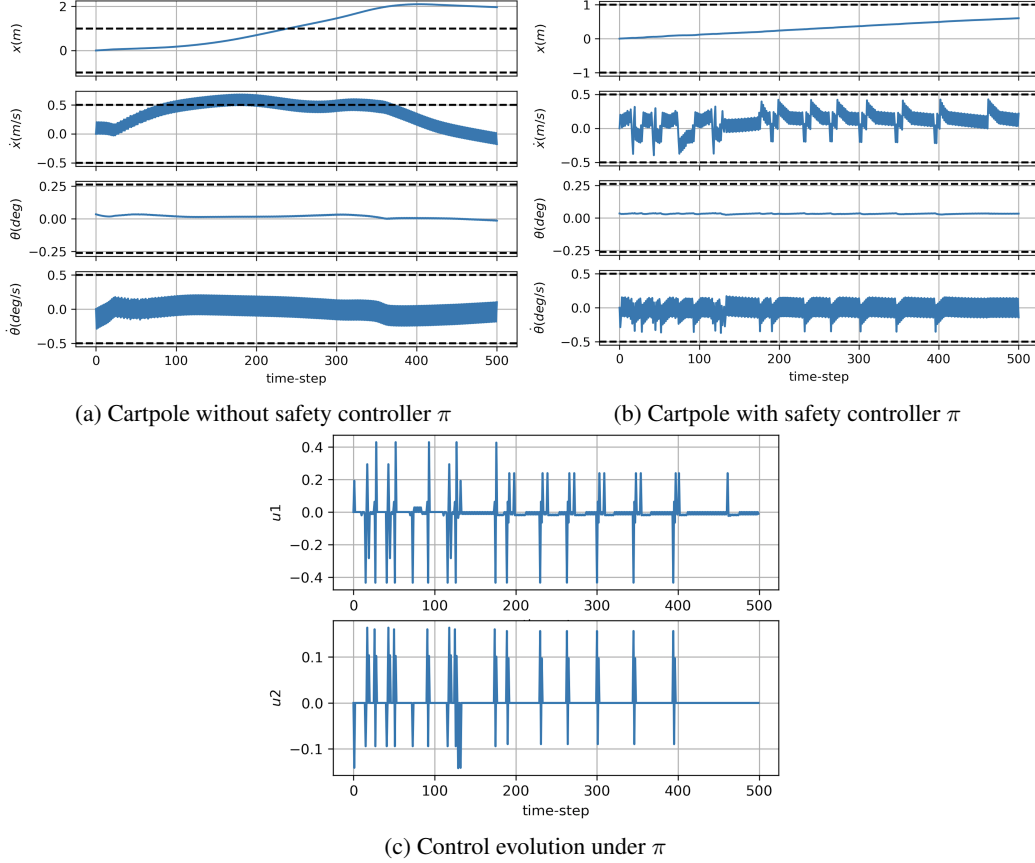


Figure 4: State evolution of the cartpole NNDM with 2 layers for 500 steps with and without safety feedback controller π in (a) and (b), respectively. Blue line shows state evolution for the system starting at $x = 0$, $\dot{x} = 0$, $\theta = 0.0349$, and $\dot{\theta} = 0$. Black dotted line demarcates the state space (X) in \dot{x} , $\dot{\theta}$, and safe space (X_s) in x and θ dimension respectively.

Cartpole For this 4-dimensional agent, we trained a NNDM that predicts the next state of the cartpole given the current state, i.e., $f^w : \mathbb{R}^4 \rightarrow \mathbb{R}^4$. For each model, we trained a NNDM, $f^w : \mathbb{R}^4 \rightarrow \mathbb{R}^4$, with one to three layers with 128 neurons in each layer. The NNDM is trained in region $x \in [-2.4, 2.4]$, $\dot{x} \in [-0.6, 0.6]$, $\theta \in [-\frac{\pi}{15}, \frac{\pi}{15}]$ and $\dot{\theta} \in [-0.6, 0.6]$. The safe set is $x \in [-1, 1]$ and $\theta \in [-\frac{\pi}{15}, \frac{\pi}{15}]$ with control limits $u_1, u_2 \in [-1, 1]$ in linear and angular acceleration dimensions. The initial set is defined to be $\theta \in [-\frac{\pi}{36}, \frac{\pi}{36}]$.

While the computation time to obtain the linear approximations increases significantly as the number of layers and number of neurons per layer increases, we notice the same trends as observed in the Pendulum agent’s experiment, i.e., an increase in P_s with finer discretization for a fixed model and a decrease in P_s as the model gets deeper (more hidden layers). For all the cartpole models, to achieve the desired probability of safety δ_s , the controller needs to be applied in all the regions. Figure 4 shows the evolution of the 2-layer NNDM cartpole with and without the safety controller. We can see that NNDM enters the unsafe space in x and \dot{x} dimensions without the controller π . But, our controller is able to keep the system within the safe set as seen in Figure 4b while it also stays within its allowable range of controller magnitude $[-1, 1]$ as seen in Figure 4c.

A.2 Husky

We trained two Husky NNDMs for a specific task using the approach outlined in [9]. Specifically, a hybrid Model-Based Model-Free (MB-MF) architecture has been used for training NNs that represent the dynamic model of the Husky robot [47]. Further, this NN with a model-based controller, i.e. Model Predictive Controller (MPC), was used to learn tasks that include moving from one point to

Table 3: State Space X for each agent of dimension n in our case-studies over which we compute linear over-and under approximation $\bar{f}_q(x)$ and $\underline{f}_q(x)$ and their corresponding extreme values in region q using the discretization $|Q|$ as mentioned in Table 2.

Model	n	State	Lower	Upper
Pendulum	2	θ	$-\pi/15$	$\pi/15$
		$\dot{\theta}$	-1	1
Cartpole	4	x	-1	1
		\dot{x}	-0.5	0.5
		θ	$-\pi/15$	$\pi/15$
		$\dot{\theta}$	-0.5	0.5
Husky	4	x	-0.5	2
		y	-1	1
		θ	$-\pi/12$	$\pi/12$
		v	-0.5	0.5
Husky	5	x	-0.5	2
		y	-0.5	0.5
		θ	$-\pi/18$	$\pi/18$
		v	-0.5	0.5
		ω	-0.5	0.5
Acrobot	6	$\cos(\theta_1)$	-0.1	0.1
		$\sin(\theta_1)$	-0.6	0.6
		$\cos(\theta_2)$	-0.1	0.1
		$\sin(\theta_2)$	-0.6	0.6
		$\dot{\theta}_1$	-0.25	0.25
		$\dot{\theta}_2$	-0.25	0.25

another, and staying in a lane. We use the data generated from this model to initialize a model-free RL algorithm to gain better sample efficiency. This enabled us to learn the unknown dynamic model and a policy for the task with less number of samples compared to a pure model-free approach.

In our case study, we first consider a 4-dimensional Husky model [47], whose states are the x and y position, the orientation θ and the velocity v . The NNDM is trained in region $x \in [-0.5, 2]$, $y \in [-1, 1]$, $\theta \in [-\frac{\pi}{12}, \frac{\pi}{12}]$ and $v \in [-0.5, 0.5]$. The control actions for this model are linear acceleration and angular velocity with control limits $u_1, u_2 \in [-1, 1]$. The initial set is any position with a circle of radius 0.1 around the origin, i.e., $x \in [-0.1, 0.1]$ and $y \in [-0.1, 0.1]$.

Further, we also train a 5-dimensional Husky model in which we observe the angular velocity ω along with linear velocity, orientation, and position as in the 4-dimensional case-study. The state space is $x \in [-0.5, 2]$, $y \in [-0.5, 0.5]$, $\theta \in [-\frac{\pi}{18}, \frac{\pi}{18}]$, $v \in [-0.5, 0.5]$, and $\omega \in [-0.5, 0.5]$. The safe set is defined over y to be $[-0.5, 0.5]$ while the control actions, control limits and the initial set remains the same.

The dynamic model has an input layer with each neuron (six for 4D Husky and seven for 5D Husky in total) representing the individual states and controls of the system. Further, the dynamic model consists of one hidden layer with 500 neurons (ReLU activation function), and the output of the NN is the state difference (4 output neurons for 4D Husky and 5 for 5D Husky) for a defined discretization time ΔT .

Training The data used for training the dynamic model was generated from the described Husky environment modelled in the PyBullet physics simulator [42]. The dynamic model is trained using trajectory data generated from PyBullet, by applying random actions to a set of initial states sampled from a distribution.

Table 4: Parameters for dynamic model and policy network training for the husky systems.

Parameter	4D Husky	5D Husky
Open-loop Dynamic Model Architecture	$6 \times 500(\text{ReLU}) \times 4$	$7 \times 500(\text{ReLU}) \times 5$
Policy Network Architecture	$4 \times 64(\tanh) \times 64(\tanh) \times 2$	$5 \times 64(\tanh) \times 64(\tanh) \times 2$
Dynamic Model Training Epoch	200	200
Discretization Time ΔT (secs)	0.1	0.1
MPC Controller Horizon (Timesteps)	1	1
Number of MPC rollouts	100	100
Closed-loop NNDM Architecture 1	$4 \times 256(\text{ReLU}) \times 4$	$5 \times 512(\text{ReLU}) \times 5$
Closed-loop NNDM Architecture 2	$4 \times 256(\text{ReLU}) \times 256(\text{ReLU}) \times 4$	-

The data is normalized to give equal weights to all the states. We used a MPC controller to generate policies required to complete the specific task. We then generated a set of expert actions from

this MPC controller to train a new policy network π_c . The policy network has one input layer (4 input neurons) representing the states, two hidden layers with 64 neurons each (all tanh activation functions), and one output layer with 2 neurons representing the actions. This policy network π_c was used as an initial policy for the model-free RL. We used the Trust Region Policy Optimization algorithm (TRPO) as a policy gradient method to perform RL. The parameters that we used for our training are described in Table 4.

The trained dynamic model and the policy network π_c were combined to represent the closed-form dynamics of the system. We performed imitation learning on the input-output data obtained from this combined model, to train a NNDM $f^w : \mathbb{R}^n \rightarrow \mathbb{R}^n$, where n is the states of the system.

A.3 Acrobot

We train a NNDM to imitate the OpenAI Gym Acrobot model under a given expert controller. The setting we consider is the same as in [48]. It is an underactuated agent (double pendulum) with control applied to the second joint. The NNDM is trained in region from $[-1, 1]$ in the first 4 dimensions, i.e., $\cos(\theta_1)$, $\sin(\theta_1)$, $\cos(\theta_2)$ and $\sin(\theta_2)$. The model was trained over 25000 data points with 300 epochs and validation loss of 10^{-3} . The state space over which the system is verified is mentioned in Table 3.

Here, θ_1 is the angle of the first joint and θ_2 is the angle relative to the angle of the first link. The task for this agent is for the tip of the second link to reach a height of $y = \sin(\theta_1) + \sin(\theta_1 + \theta_2) = 1$. A safety constraint is added such that the tip of the second link should not go beyond $y = 1.2$, i.e., $\sin(\theta_1) \leq 0.6$ and $\sin(\theta_2) \leq 0.6$. Hence, the safe set is defined as $\sin(\theta_1) \in [-0.6, 0.6]$ and $\sin(\theta_2) \in [-0.6, 0.6]$. Note, the maximum height the pendulum can reach is 1.8 m. Finally, the initial set is defined to be any initial point within a radius of 0.1 around the origin in the first 4 dimensions.